1

Introduction

The most visible effects of earthquakes are their impacts on natural and man-made structures at the Earth's surface. The transfer of energy from the source that causes the destruction takes place through the agency of seismic waves. These same waves travel out through the Earth to be recorded at distant locations using sensitive seismographs. In their passage through the Earth the waves acquire characteristics related to the properties of the regions through which they have travelled. Our knowledge of the interior structure of the Earth derives in large part from the unravelling of the different influences on the character of the seismic wavefield.

For the large scale structure of the Earth, the major source of information comes from the records of ground motion produced by the waves from earthquakes at seismic stations across the globe. At smaller scales man-made sources become important. Most of the knowledge of the seismic wavespeeds in the crust and the uppermost mantle is derived from observations of reflected and refracted waves on networks of seismic instruments specifically deployed for structural studies. In exploration work, particularly for petroleum, all the information comes from complex observational procedures in which attention is focussed on those parts of the seismic wavefield whose propagation paths are close to vertical.

The interpretation of seismic records requires an understanding of the generation and propagation of the seismic waves and the influence of the recording process, since each imposes its imprint on the seismogram. Improvements in the quality of seismic instrumentation mean that it is now possible to obtain a faithful rendition of the particle motion at the seismic sensor in digital form over a broad range of frequencies. The use of broad-band data requires careful attention to the nature of the disorganised component of seismic motion, commonly known as *noise*. It is against the background of seismic noise that the arrivals of interest have to be sought.

1.1 Seismic signals

The surface of the Earth is in constant slight movement which can be detected with a sensitive seismometer. The ground motion arises from both local effects, such as

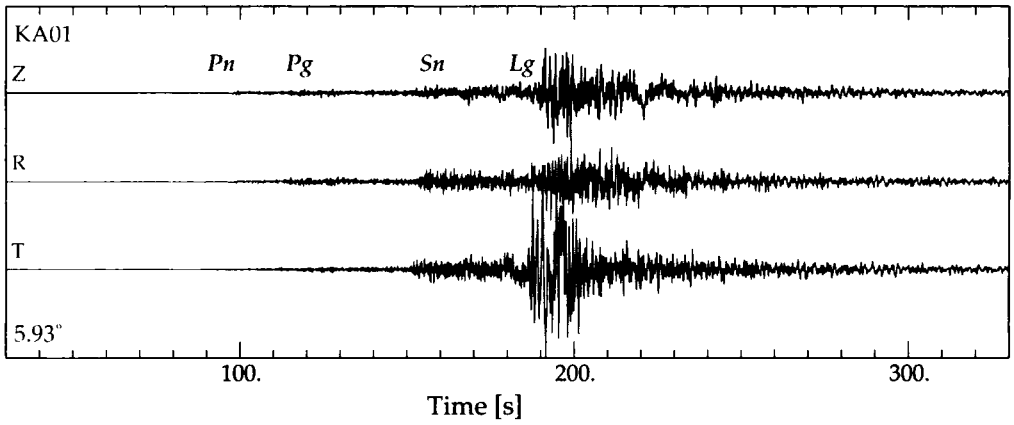

Figure 1.1. Unfiltered three-component velocity records from a portable broad-band recording system for a large local event (Mb = 6.3) in NW Australia at an epicentral distance $\Delta = 5.93°$. The horizontal component traces have been rotated to align along (R) and transverse (T) to the propagation path.

man-made disturbances or the rocking of trees in the wind, and vibrations induced by distant processes such as the microseisms generated by distant storms in the ocean.

From time to time the irregular pattern of ground motion is interrupted by an organised pattern of energy which rises above the background (figures 1.1, 1.2). Such well-defined wavetrains are induced by the excitation of seismic waves by a natural or artificial source and their subsequent propagation through the earth to the recording site. The two seismograms in figure 1.1 and figure 1.2 have been recorded at nearby sites in northwestern Australia in a deployment of portable broad-band seismic instrumentation. They show the major differences in the appearance of the seismic wavetrain with distance from the source. Figure 1.1 shows the three-orthogonal components of ground velocity at a distance of about 660 km from a relatively large local event (Mb 6.3); whereas figure 1.2 shows comparable records for a shallow event near the Fiji Islands at a distance of 5685 km from the source.

The characteristic form of the the wavetrain in each case includes a number of distinct arrivals associated with particular propagation paths, which have a more distinct pulse-like appearance at the larger distance. The distinct arrivals are accompanied by a lower level 'coda' arising from the superposition of many different processes and the influence of scattering. Following the initial group of body-wave phases such as *P*, *S*, the amplitude of the records increases as a sequence of waves arrives which have been guided by the presence of the Earth's surface (*Lg* in figure 1.1, *Love*, *Rayleigh* in figure 1.2). These surface waves have a more limited penetration into the Earth than the body waves and have somewhat lower frequencies. The difference in frequency is small for the shorter distance of propagation in figure 1.1 but is much more apparent in figure 1.2 where the long-period undulation associated with the

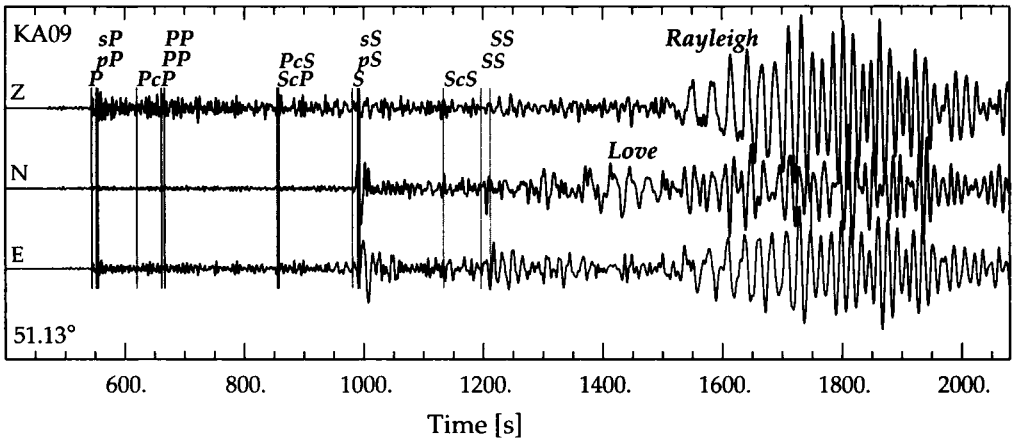

Figure 1.2. Unfiltered three-component velocity records from a portable broad-band recording system in NW Australia for a shallow event near the Fiji islands at an epicentral distance Δ = 51.13°. The event is almost due east of the receiver so the horizontal components are naturally polarised with transverse motion to the path on the N/S component.

surface waves is very distinct. In later chapters we will follow the development of the seismic wavefield and show how seismograms such as those displayed in figures 1.1 and 1.2 attain their form.

The most common natural generators of seismic waves are earthquakes associated with tectonic processes which can impart substantial energy in the form of seismic waves. In the period range from 0.001 Hz to 4 Hz the seismic waves from earthquakes can be detected at considerable ranges from the source (e.g. with a surface displacement of around 10^{-8} m at 9000 km for a surface wave magnitude of 4). For the largest earthquakes, wavetrains can be observed which have circled the globe a number of times.

The largest earthquakes have a tectonic character and involve substantial displacement on a fault surface. These relatively rare events are accompanied by very large numbers of smaller events. Nearly all large events are followed by a set of smaller earthquakes in the same region. These aftershocks appear to be related to the fault plane that slipped during the large event, but can also occur on nearby fault systems which have been activated by the redistribution of stresses following the main event. The aftershocks normally have significantly lower magnitude than the main event and decay fairly rapidly with time. The largest aftershocks, which occur soon after the event, can have a significant effect because of their interactions with structures which have been damaged by the large event. The distribution of aftershocks is often used to infer both the fault area and to provide information on the distribution of the slip in the rupture associated with the main event. Aftershocks often seem to concentrate around regions with lower slip which are termed asperities.

The most common natural generators of seismic waves are earthquakes associated

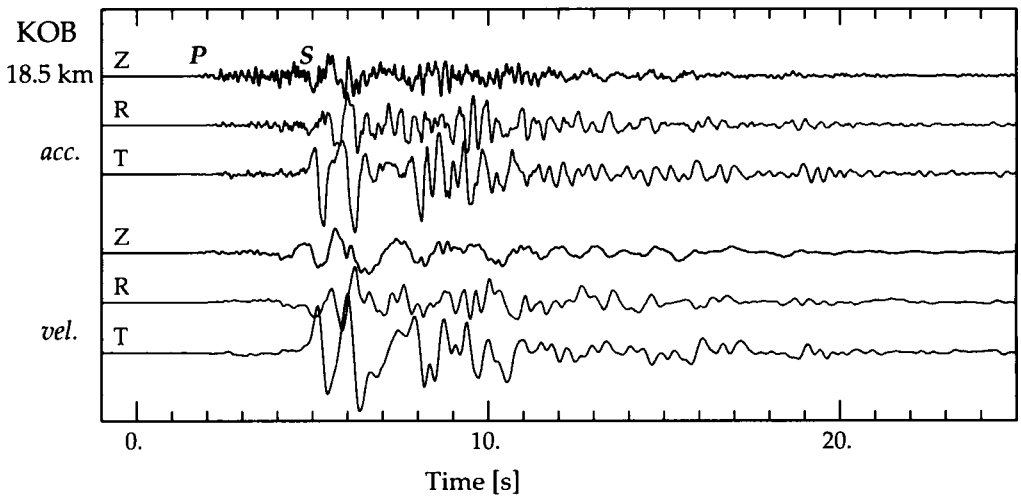

Figure 1.3. Three-component records for the KOB accelerometer in the city of Kobe, Japan for the 1995 Hyogo-ken Nanbu (Kobe) earthquake (Mw 6.9) which devastated the city. The station was about 19 km from the epicentre of the earthquake and the traces are rotated so that the horizontal components aligned along (R) and perpendicular (T) to the path from the epicentre. The ground velocity records obtained by integrating the accelerograms are also shown. The records are dominated by *S* waves with a long duration arising in part from the complex rupture pattern of the event. [Data courtesy of the Japan Meteorological Agency].

with subduction processes. However, sizeable events have occurred in continental regions well away from any tectonic boundary, as for example the sequence of three Mb 6 events within 12 hours in 1988 near Tennant Creek in the Northern Territory of Australia (see, e.g., Bowman et al, 1990). Many volcanoes also show associated earthquake activity which may, for example, arise from rapid magma transport or motions on faults above a magma chamber.

In the immediate neighbourhood of a large earthquake the Earth's surface suffers very large ground motion which is sufficient to overload many seismic instruments. In regions with a high incidence of earthquakes, such as California and Japan, specially emplaced accelerometer systems are installed to record these very large motions. The recordings are normally triggered by the arrival of the compressional *P* waves and modern systems have an extended data buffer, so that at close ranges the onset can be captured as well as the *S* waves and surface waves. In figure 1.3 we illustrate such strong ground motion with the record from the accelerometer operated by the Japan Meteorological Agency in the city of Kobe, Japan for the major earthquake in 1995 (Mj 7.2) which devastated the city. The station was about 19 km from the epicentre of the earthquake. The faulting pattern was complex with multiple subevents and rupture on both sides of the focus leading to prominent surface faulting in Awaji Island to the south and major destruction in the city of Kobe itself (Yoshida, 1996). Complex 3-dimensional structure beneath the city tended to reinforce the ground motion near

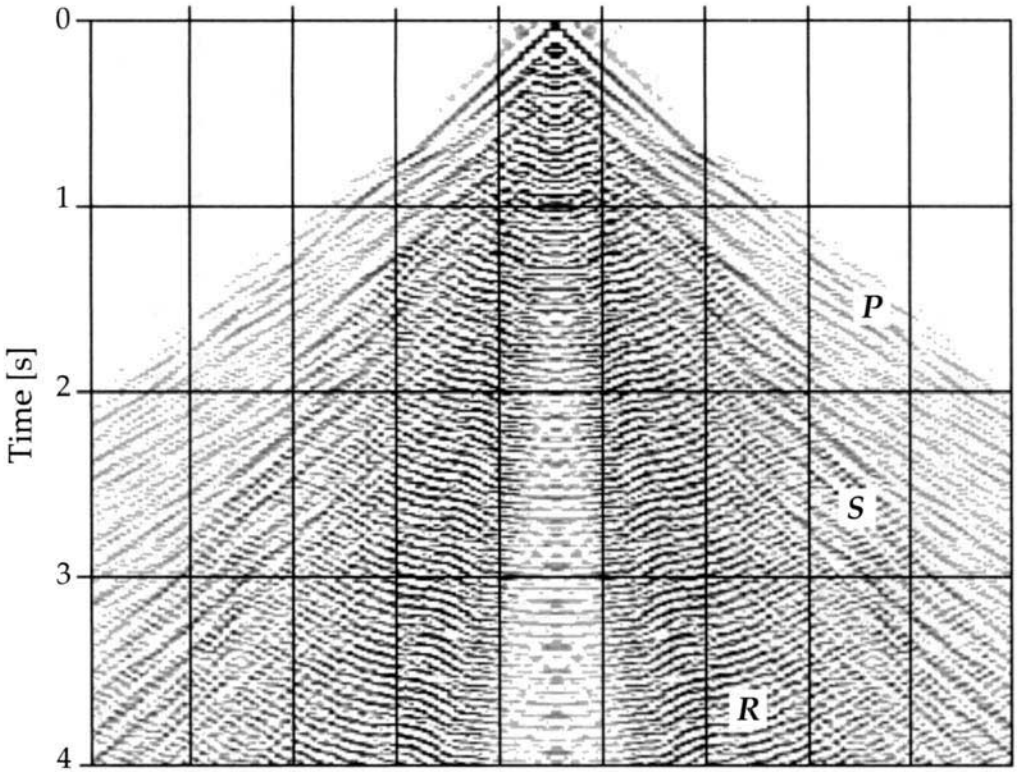

Figure 1.4. Land reflection spread on land from a vibrator source on a complex layered structure, showing prominent *P* reflections and refractions as well as *S* wave and Rayleigh wave (*R*) arrivals.

the fault line, leading to major damage (Koketsu & Furumura, 1998). Figure 1.3 shows both the original accelerometer records and the ground velocity derived by integration. The initial high frequency *P* waves are followed closely by large amplitude *S* waves which are particularly prominent on the tangential component to the path to the epicentre (T) on which horizontally polarised *SH* waves are expected. The complexity of the *S* wave records reflects the rupture process in the earthquake as well as the local structure.

Most man-made sources of seismic energy such as chemical explosions, surface vibrators or weight-dropping devices have a limited range over which they give detectable arrivals. This distance is about 2 km for a single surface vibrator and may be as large as 1000 km for a charge of several tons of TNT. Only large nuclear explosions rival earthquakes in generating seismic waves which are observable over a considerable portion of the Earth's surface.

Three examples of man-made seismic signals are shown in figures 1.4–1.6, from exploration seismology, large-scale refraction seismology and recordings of an underground nuclear test.

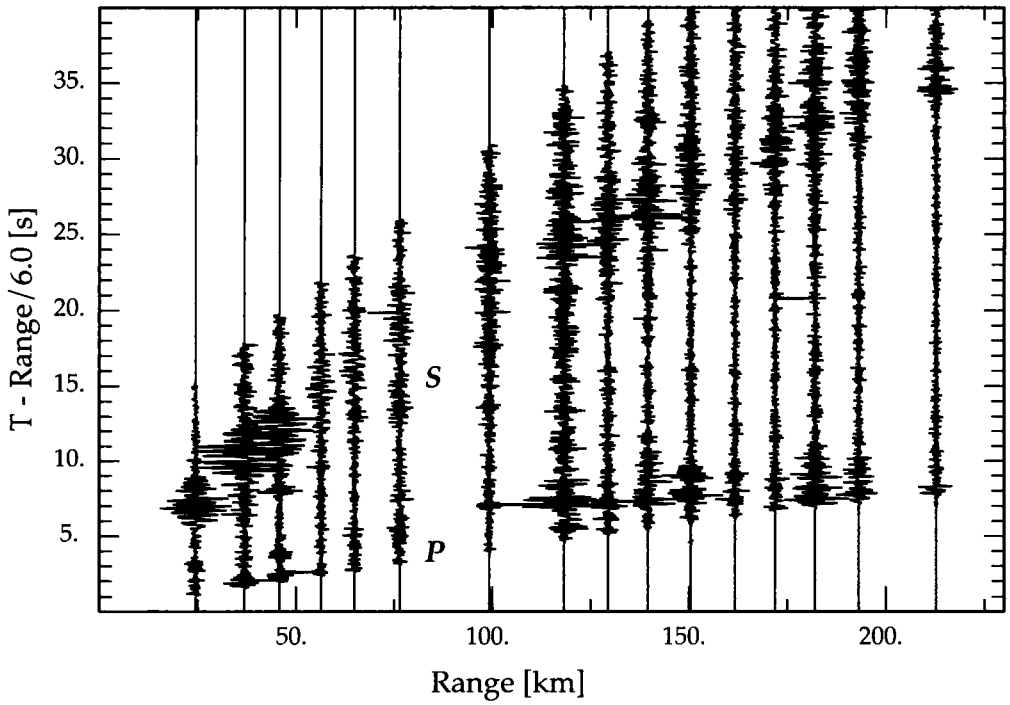

Figure 1.5. Radial component records for short distances from shotpoint B of the Fennolora seismic refraction experiment [courtesy of University of Karlsruhe].

The exploration example (figure 1.4) shows a 4 km spread from vibrator sources over complex layered horizons. The vibrators produce significant radiation in the form of vertically directed compressional (*P*) waves, but also shear waves radiated at about 45 degrees to the vertical. The source lies at the surface and so a large fraction of the radiated energy is carried as fundamental mode Rayleigh waves. These effects can be clearly seen in figure 1.4. The onset of *P* waves with prominent refractions is clear, and the associated reflections can be tracked back towards short offsets, but at larger times the *P* arrivals tend to be masked by other arrivals such as *S* waves and Rayleigh waves (*R*). The object of seismic processing in exploration is to extract the reflection signal which contains the major part of the geological information. The other arrivals whose properties are controlled by the shallow part of the layering are less used; although *P* information is sometimes used to build corrections for variations in the wavespeed in the near-surface layers.

The second example is taken from investigations of the structure of the Earth's crust and uppermost mantle where attention is concentrated on the body wave portion of the wavefield. Figure 1.5 shows radial component records from a small portion of the FENNOLORA project, a major long-range refraction profile through Sweden and northern Finland. The source for these records was an explosion in shallow water

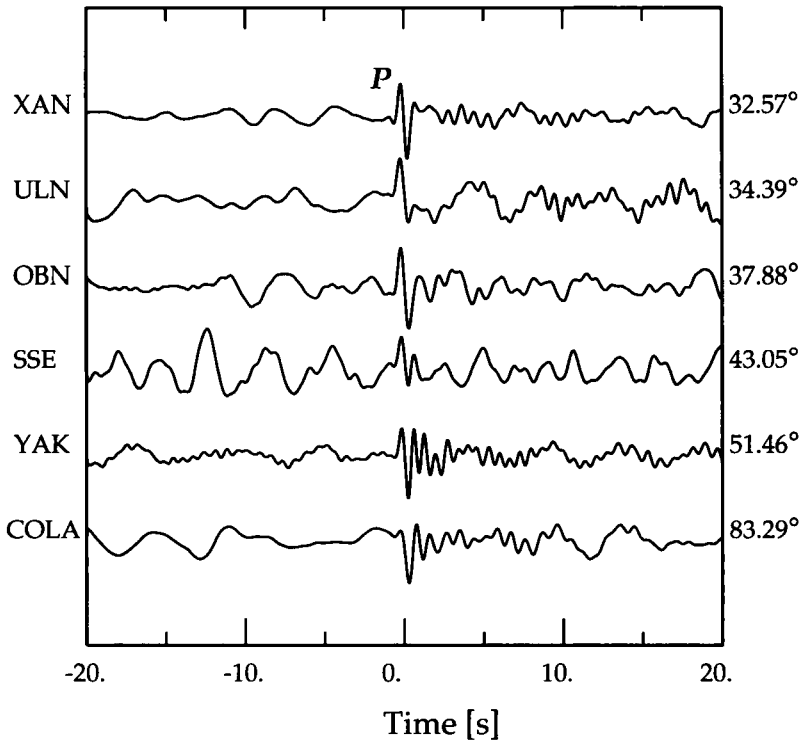

Figure 1.6. Vertical component *P* wave records from the Indian nuclear test of 1998 May 11 recorded at teleseismic broadband stations. The records are aligned on the onset of *P*.

and the seismometer component represents horizontal motion along the line of the profile. The group of records has been shifted in time with distance so that we can follow the earliest *P* waves, and reduce the total time span to be displayed. Very clear *P* and *S* wave signals are seen, with quite complex character associated with crustal propagation. There is a prominent *P* reflection from the crust-mantle boundary near a reduced time of 8 s for ranges beyond 100 km. The explosive source generates only *P* waves so all the *S* wave energy has been produced by wavetype conversion.

The final example (figure 1.6) shows the records of *P* waves produced by underground nuclear test in northwestern India on 1998 May 11 at teleseismic distances at a number of broadband stations around the globe (the epicentral distances in degrees are indicated at the right). There is a sharp simple *P* pulse which is very consistent between stations. No significant *S* waves can be found in the records; this is consistent with the simple model of an expanding pressure pulse source from the nuclear explosion.

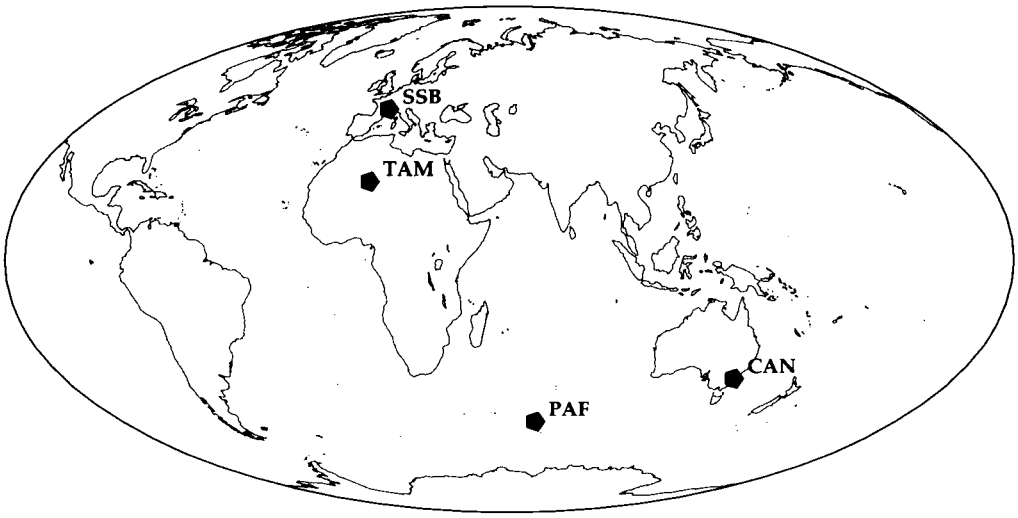

Figure 1.7. GEOSCOPE stations selected for display of the seismic noise spectrum.

1.2 Seismic noise

The nature of the seismic noise spectrum has had a profound influence on the nature of the instruments which have been developed to record earthquake signals and this in turn has affected the way in which seismic wave theory has developed.

There are a wide range of contributions to the background noise including the presence of tides, atmospheric pressure, diurnal effects mostly associated with temperature variation, and human-induced activity. Although efforts are made to place permanent seismic instruments in quiet locations away from sources of potential noise, long-established sites frequently suffer from increased noise due to encroachment of human activity as cities expand.

The noise pattern is dominated by a strong noise peak for frequencies from 0.09–0.18 Hz which arises from the influence of microseisms which mostly arise from standing waves induced by storms in the deep ocean. Wave surf can also be significant in the frequency range 0.05–0.10 Hz. The level of microseismic noise therefore depends on the season and is of most significance for stations close to the ocean. Mid-continental stations generally have conditions with somewhat lower noise levels.

We illustrate the influence of station location with noise spectra for the year 1995 taken from a number of stations in the GEOSCOPE network (figure 1.7). We display spectra taken at the mid-continental site TAM in Algeria, SSB in central France, CAN about 160 km from the coast of southeastern Australia and the island station PAF in the Kerguelen islands (figure 1.8). Each station uses Streckeisen STS-1 broad-band sensors with a comparable recording system. The power spectral density for acceleration is

displayed for each of the three components at the stations, by combining results for different recording bands. The units are decibels, i.e. $10\log_{10}$(signal power), so that a variation of 20 dB corresponds to a factor of 10 variation in ground acceleration. The dashed lines shown in each of the frames of figure 1.8 represent the high- and low-noise models developed by Peterson (1993). In favourable circumstances the noise levels on the vertical component instruments can approach the low-noise floor.

The variation of the noise levels near the microseismic peak exceeds 36 dB, with nearly a factor of 100 in acceleration. The levels at this peak and in the high frequency range are normally comparable for each of the three-components. But, as can be seen from figure 1.8, the noise levels at long periods for horizontal component instruments are somewhat higher than for the vertical component. A major influence on the long period noise level is atmospheric pressure. Slight variations of pressure induce ground tilting which is only recorded on the horizontal components.

The energy release from earthquakes spans an enormous range. The waves generated by the smallest events lie well below the detection threshold of even the most sensitive seismometers. The largest events produce very strong ground motion in their immediate vicinity. A seismic recording system thus requires a large dynamic range to cope with the range of conditions that may be experienced.

The strong variation in noise level with frequency and station location means that the detection capability for seismic signals of interest differs dramatically depending on the nature of the disturbance. Long period surface waves from an event may well rise above the noise even though the shorter period body waves are submerged in the ambient ground motion. At an island station such as PAF, it will not be possible to detect seismic signals from events which would be readily recorded on a mid-continental station such as TAM at a comparable distance from the source.

The seismic noise spectrum is not static but varies on both a daily and seasonal basis as illustrated in figure 1.9 for station SSB in France. The daily variations lead to enhanced high frequency noise in daylight hours, much of which is due to increased human activity during the day, but also to the higher temperatures and larger atmospheric variations during the day. The seasonal variations correlate with the presence of stronger storm systems in the North Atlantic in the winter which raise the level of the microseismic peak noticeably.

Such seasonal variations can be particularly severe for stations with climates with a very strong contrast between winter and summer. Stations in the northern land masses can be very quiet in winter when the whole area is frozen and there is a snow blanket, but the spring thaw can bring much higher noise particularly when stations lie near a body of water.

Details of the method used for noise estimation and a discussion of noise conditions at the full range of GEOSCOPE stations for the year 1995 can be found in Stutzman, Roult & Astiz (2000).

The major noise peaks associated with the microseisms at 0.09–0.18 Hz caused

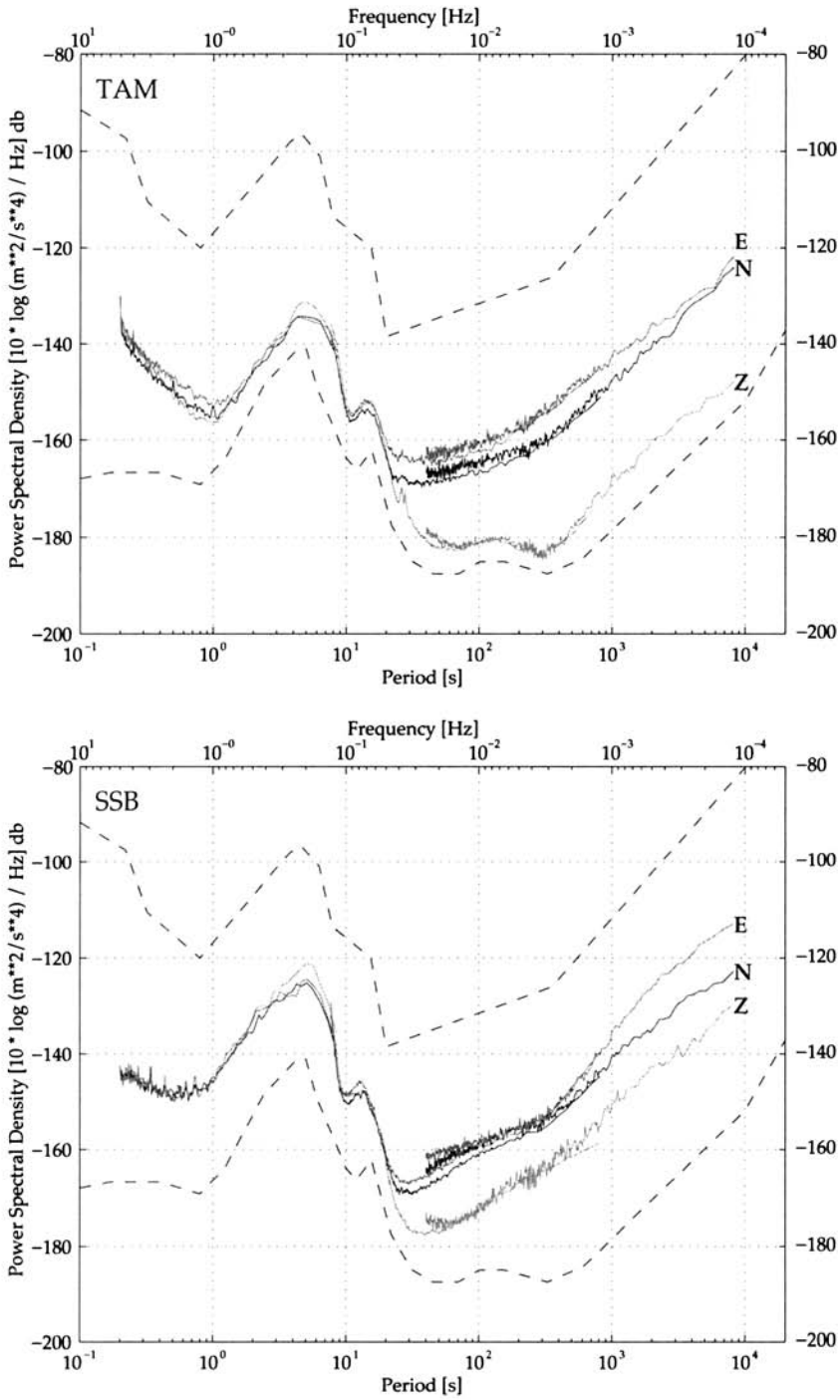

Figure 1.8. Power spectral density for acceleration at the Earth's surface. The upper and lower dashed curves represent the high- and low-noise model of Petersen (1981). (a) TAM: Tammanraset, Algeria, (b) SSB: St Saveur, France [courtesy of GEOSCOPE].